



Cite this: *Phys. Chem. Chem. Phys.*,
2015, 17, 31011

Photoelectron spectroscopy and density functional calculations of $C_nS_m^-$ ($n = 2-7$; $m = 1, 2$) clusters†

Xi-Ling Xu, Xiao-Jiao Deng, Hong-Guang Xu and Wei-Jun Zheng*

$C_nS_m^-$ ($n = 2-7$; $m = 1, 2$) clusters were investigated by using photoelectron spectroscopy combined with density functional theory calculations. We found that the vertical detachment energies of both C_nS^- and $C_nS_2^-$ ($n = 2-7$) clusters exhibit a strong odd–even alternation with an increasing number of carbon atoms: the VDEs of even- n clusters are higher than those of adjacent odd- n clusters. The most stable structures of the anionic and neutral C_nS ($n = 2-7$) clusters are linear with the S atom locating at one end of the carbon chain except that the structure of C_3S^- is slightly bent. The ground state isomers of the anionic and neutral C_nS_2 ($n = 2-7$) clusters are all linear structures with two S atoms locating at two ends of the carbon chain. The electron affinities of the neutral C_nS ($n = 2, 4-7$) and C_nS_2 ($n = 2-7$) clusters are determined based on the experimental adiabatic detachment energies of the corresponding anion species, because the most stable structures of the neutral clusters are similar to those of the corresponding anions.

Received 30th July 2015,
Accepted 27th October 2015

DOI: 10.1039/c5cp04482k

www.rsc.org/pccp

1. Introduction

Both carbon and sulfur are among the most abundant elements in circumstellar and interstellar environments and thus play vital roles in astrochemical processes. Carbon atoms are ubiquitous in our daily life. Sulfur is also an essential element for all lives. Sulfur compounds largely exist in oil, animals, and plants.^{1,2} A series of linear pure carbon clusters C_n ($n = 2, 3$, and 5) have been detected in the interstellar medium by means of radio astronomy.³⁻⁵ C_{60} and C_{70} have also been observed in a young planetary nebula (Tc 1) by their IR spectra.⁶ In the past decades, the sulfur-containing carbon chains C_nS_m ($m = 1, 2$) have attracted broad attention due to the fact that C_nS ($n = 1-3, 5$) molecules were identified in various interstellar medium (ISM) objects, such as the cold molecular clouds OMC-1 and TMC-1, the circumstellar envelopes of protostellar B335 and carbon-star IRC+10216 through radio astronomy.⁷⁻¹⁴ Although the SC_nS species are undetectable in the ISM *via* radio astronomy because of their zero dipole moments, they may be observable by their IR absorption.

To understand the structures and properties of C_nS_m clusters and to provide useful data for astronomical observations, scientists have extensively investigated C_nS_m ($m = 1, 2$) clusters both experimentally and theoretically. Small C_2S and C_3S clusters have been studied by several research groups using

microwave spectroscopy,^{11,15-17} matrix isolation infrared absorption spectroscopy,¹⁸⁻²⁰ and laser induced fluorescence spectroscopy.^{21,22} Vala group investigated C_nS ($n = 1-6$) and C_nS_2 ($n = 1-5, 7, 9, 11, 13, 15$) clusters using Fourier transform infrared absorption spectroscopy in the Ar matrix.^{23,24} Neumark and coworkers investigated the photoelectron spectra of C_2S^- and C_3S^- using slow photoelectron velocity-map imaging spectroscopy (SEVI) and obtained the gas phase vibrational frequencies and electron affinities of C_2S and C_3S .^{25,26}

The doping of carbon clusters with sulfur atom(s) has received much attention also because the addition of sulfur atom(s) could improve the stabilization of the carbon chain. As we all know, the stable structures of the pure C_n clusters are changing from linear with $n \leq 9$ to ring with $n \geq 10$, to cage structure with a larger size.^{27,28} However, Wang *et al.* predicted that the stable structures of C_nS_m ($m = 1, 2$) can maintain the linear configurations with up to 29 carbon atoms using B3LYP/6-311G* methods.²⁹ Wang *et al.* also calculated the vibrational absorption spectra of linear C_nS ($n = 2, 6$) and C_nS_2 ($n = 7, 9, 11, 13, 15$) clusters using the same method.²⁴ Pascoli and Lavendy studied the structures and energies of C_nS ($n = 1-20$) and C_nS^+ ($n = 1-23$) clusters by means of density functional theory (DFT).^{30,31} They found that the energetically most favorable isomers of C_nS are linear structures with the sulfur atom at the very end of the carbon chain except that the $C_{18}S$ is predicted to have a S-capped monocyclic structure with a low barrier to linearity. Tang and Bel Bruno calculated the structures and energies of C_nS^+ ($n = 1-16$) and C_nS^- ($n = 9-16$) using the DFT method.³² Lee and coworkers investigated the structures and spectroscopic properties of linear C_nS ($n = 2-9$) and C_nS_2 ($n = 2-6$) using DFT

Beijing National Laboratory for Molecular Sciences, State Key Laboratory of Molecular Reaction Dynamics, Institute of Chemistry, Chinese Academy of Sciences, Beijing 100190, China. E-mail: zhengwj@iccas.ac.cn; Fax: +86 10 62563167; Tel: +86 10 62635054

† Electronic supplementary information (ESI) available. See DOI: 10.1039/c5cp04482k

calculations.^{33,34} Pérez-Juste *et al.* examined the electronic structure of linear sulfur-carbon chains C_nS ($n = 1-6$) by means of several theoretical methods.³⁵ Zhang *et al.* investigated the structures and stabilities of linear carbon chains C_nS ($n = 1-10$) in their ground states by the CCSD and B3LYP approaches.^{36,37}

For larger C_nS with $n \geq 4$ and C_nS_2 , there is no report about their anion photoelectron spectroscopy. In order to explore the electronic and geometric structures of $C_nS_m^-$ ($n = 2-7$; $m = 1, 2$) clusters and to provide useful information for future high-resolution spectroscopy studies, in this work, we investigated $C_nS_m^-$ ($n = 2-7$; $m = 1, 2$) clusters using photoelectron spectroscopy and DFT calculations.

2. Experimental and theoretical methods

2.1. Experimental method

The experiments were performed using a home-made apparatus consisting of a laser vaporization source, a time-of-flight (TOF) mass spectrometer, and a magnetic-bottle photoelectron spectrometer, which has been described previously.³⁸ Briefly, the $C_nS_m^-$ ($m = 1, 2$) cluster anions were produced in the laser vaporization source by ablating a rotating and translating disk target (13 mm diameter, C:S mole ratio 4:1) with the second harmonic (532 nm) light pulses from a nanosecond Nd:YAG laser (Continuum Surelite II-10). Helium gas at a 4 atm backing pressure was allowed to expand through a pulsed valve (General Valve Series 9) into the source to cool the formed clusters. The generated cluster anions were mass-analyzed using the TOF mass spectrometer. The cluster anions of interest were mass-selected and decelerated before being photodetached by another Nd:YAG laser (Continuum Surelite II-10, 266 nm). The photodetached electrons were energy-analyzed by the magnetic-bottle photoelectron spectrometer. Photoelectron spectra were calibrated using the spectra of Cu^- and Au^- taken under similar conditions. The resolution of the photoelectron spectrometer was approximately 40 meV for electrons with 1 eV kinetic energy.

2.2. Theoretical method

The structures of $C_nS_m^-$ ($n = 2-7$; $m = 1, 2$) clusters and their neutral counterparts were optimized using DFT with the Becke's three-parameter and Lee-Yang-Parr's gradient-corrected correlation hybrid functional (B3LYP).^{39,40} The 6-311+G(3d) basis set is used for both C and S. All calculated energies were corrected by the zero-point vibrational energies (ZPEs). To evaluate the accuracy of the B3LYP/6-311+G(3d) method, we also calculated the single-point energies and vertical detachment energies (VDEs) of the small size C_nS^- ($n = 2-4$) clusters using the coupled-cluster method including a full treatment singles and doubles and triple excitations non-iteratively [CCSD(T)]⁴¹ with the aug-cc-pVTZ basis set.⁴² The results obtained from the B3LYP method are very close to those from the CCSD(T) method (see Table S1 in the ESI†). Because the CCSD(T)/aug-cc-pVTZ method is much more expensive than the B3LYP/6-311+G(3d) method, here we chose the B3LYP/6-311+G(3d) method for the calculations in this work.

All the geometry optimizations were conducted without any symmetry constraint. Harmonic vibrational frequencies were calculated to confirm that the optimized structures correspond to real local minima. The theoretical VDE was calculated as the energy difference between the neutral and anionic clusters at the geometry of the anion species. The theoretical adiabatic detachment energy (ADE) was obtained as the energy difference between the neutral and the anionic clusters with the neutral structure relaxed to the nearest local minima related to the geometry of the anion. All theoretical calculations in this work were performed using Gaussian 09 program package.⁴³

3. Results and discussion

3.1. Experimental results

Fig. 1 shows a typical mass spectrum of cluster anions generated in our experiments. The major series of the mass peaks are those of C_n^- ($n = 5-13$) and S_n^- ($n = 2-4$) while the minor series are those of C_nS^- ($n = 2-10$) and $C_nS_2^-$ ($n = 1-7$). The assignments of the mass peaks were carefully confirmed by the natural isotopic distributions of the C and S elements. The ion intensities of C_nS^- and $C_nS_2^-$ are high enough for us to proceed with the photoelectron spectroscopic study although their mass peaks are relatively weak compared with those of C_n^- and S_n^- .

The photoelectron spectra of C_nS^- and $C_nS_2^-$ ($n = 2-7$) taken with 266 nm (4.661 eV) photons are shown in Fig. 2. The VDEs and the ADEs of these clusters as estimated from the photoelectron spectra are summarized in Table 1. The VDE of each cluster was taken from the maximum of the first peak in its spectrum. The ADE of each cluster can be obtained by adding the instrumental resolution to the onset of the first peak in its spectrum. The onset of the first peak was determined by drawing a straight line along the leading edge of that peak across the spectrum baseline.

C_nS^- ($n = 2-7$). The spectrum of C_2S^- contains four major bands centered at 2.75, 3.18, 3.44 and 3.98 eV, respectively. The distances of the bands at 3.18, 3.44 and 3.98 eV to the first band

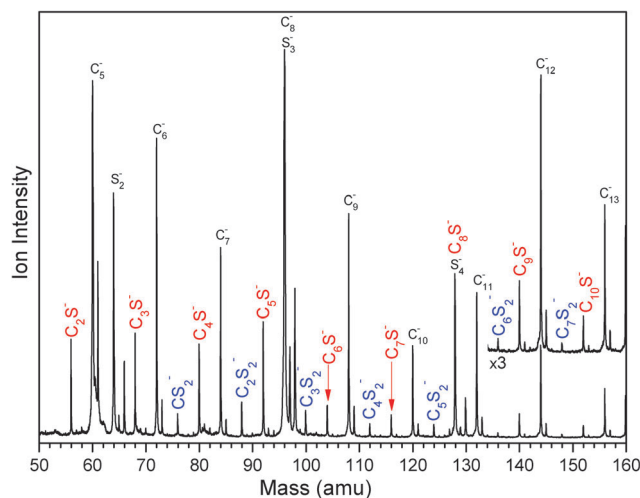


Fig. 1 Mass spectrum of C_nS^- and $C_nS_2^-$ ($n = 2-7$) cluster anions.

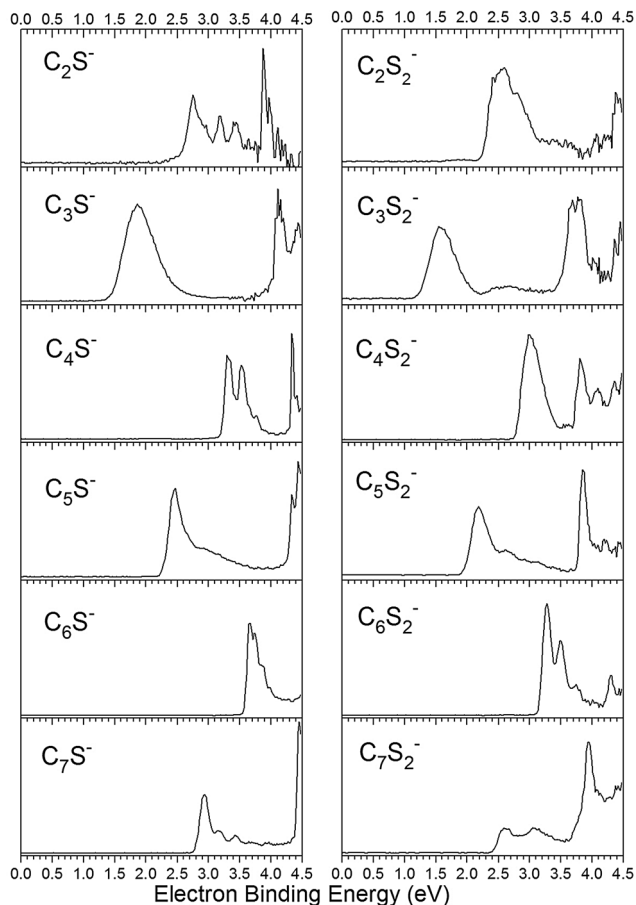


Fig. 2 Photoelectron spectra of C_nS^- and $C_nS_2^-$ ($n = 2-7$) clusters recorded using 266 nm photons.

Table 1 Vertical detachment energies (VDEs) and adiabatic detachment energies (ADEs) of C_nS^- and $C_nS_2^-$ ($n = 2-7$) clusters estimated from their photoelectron spectra

Cluster	VDE (eV)	ADE (eV)	Cluster	VDE (eV)	ADE (eV)
C_2S^-	2.75 ± 0.08	2.56 ± 0.08	$C_2S_2^-$	2.58 ± 0.08	2.27 ± 0.08
C_3S^-	1.88 ± 0.08	1.45 ± 0.08	$C_3S_2^-$	1.58 ± 0.08	1.26 ± 0.08
C_4S^-	3.32 ± 0.08	3.23 ± 0.08	$C_4S_2^-$	3.00 ± 0.08	2.79 ± 0.08
C_5S^-	2.47 ± 0.08	2.29 ± 0.08	$C_5S_2^-$	2.18 ± 0.08	1.99 ± 0.08
C_6S^-	3.65 ± 0.08	3.61 ± 0.08	$C_6S_2^-$	3.27 ± 0.08	3.18 ± 0.08
C_7S^-	2.93 ± 0.04	2.93 ± 0.04	$C_7S_2^-$	2.62 ± 0.08	2.44 ± 0.08

are 0.43, 0.69, and 1.13 eV respectively, in good agreement with the high-resolution slow photoelectron imaging spectroscopy results (0.4501, 0.7372, and 1.1275 eV) reported by Neumark and coworkers.²⁵ The band at 3.98 eV is split into three resolved peaks centered at 3.88, 3.99, and 4.10 eV, respectively, which can be tentatively assigned to the transitions from the ground state ($X^2\Pi$) of C_2S^- to the vibrational progression of the electronic excited state ($A^3\Pi$) of neutral C_2S . The separation of these three resolved peaks is about 0.11 eV ($887 \pm 100 \text{ cm}^{-1}$), which is in agreement with the vibrational frequencies of C_2S $^3\Pi_2 \nu_3$ mode (807 cm^{-1}) and $^3\Pi_1 \nu_3$ mode (803 cm^{-1}).²⁵ The spectrum of C_3S^- has two parts, the first one is a rather broad band centered at 1.88 eV, indicating a large geometry change

between the anion and the neutral, and the second one has two peaks centered at 4.16 and 4.42 eV. The broad unresolved band at 1.88 eV corresponds to the spectrum of C_3S^- reported by Neumark and coworkers,²⁶ in which there are three vibrational progressions with the frequencies of 109, 581, and 935 cm^{-1} . C_4S^- has two major bands, the first one centered at 3.50 eV is split into three peaks centered at 3.32, 3.54, and 3.76 eV, and the second one has a sharp peak centered at 4.34 eV. As we will discuss later, the first three peaks in the experimental spectrum of C_4S^- may be contributed by the low-lying electronic states and vibrational progressions of neutral C_4S .

As for C_5S^- , it has a peak centered at 2.47 eV and a long tail at the high binding energy side, followed by two peaks at 4.34 and 4.44 eV. The long tail is probably because there are unresolved vibrational states. In the spectrum of C_6S^- , there is one band, which is split into four peaks centered at 3.65, 3.75, 3.87, and 3.98 eV, respectively. Similar to C_4S^- , the four peaks may be contributed by the low-lying electronic states and vibrational progressions of neutral C_6S . For C_7S^- , there are three resolved peaks centered at 2.93, 3.18, and 3.43 eV in the low binding energy, and an additional band beyond 4.3 eV. The three resolved peaks can be tentatively assigned to the vibrational progression related to the transition from the ground state ($X^2\Pi$) of the C_7S^- anion to the electronic ground state ($X^1\Sigma^+$) of neutral C_7S . The spacing of the vibrational progression is about 0.25 eV ($2016 \pm 200 \text{ cm}^{-1}$), which is in agreement with the vibrational frequency (2088.1 cm^{-1}) of neutral C_7S measured by Wang *et al.*⁴⁴ The first peak at 2.93 eV comes from the $C_7S (\nu' = 0) \leftarrow C_7S^- (\nu'' = 0)$ transition, which stands for the ADE of C_7S^- or the electron affinity (EA) of neutral C_7S . In addition, because it is the most intensity one of the vibrational peaks, it also is the VDE of the C_7S^- anion.

$C_nS_2^-$ ($n = 2-7$). The spectrum of $C_2S_2^-$ exhibits two major bands with the first one centered at 2.58 eV and the other one beyond 4.00 eV. The band at 2.58 eV has two small shoulders at 2.41 and 2.79 eV, respectively. The spectrum of $C_3S_2^-$ has a broad band centered at 1.58 eV and a broad weak band centered at 2.64 eV, followed by one band centered at 3.74 eV and two peaks centered at 4.36 and 4.45 eV respectively. The band at 3.74 eV is split into two peaks centered at 3.67 and 3.79 eV. In the spectrum of $C_4S_2^-$, there is an intense band centered at 3.00 eV and a weak feature at 3.60 eV, followed by three other peaks centered at 3.81, 4.09 and 4.36 eV respectively.

$C_5S_2^-$ contains two major features in the ranges of 1.90–3.50 and 3.75–4.50 eV, in which the feature at the low electron binding energy side has one sharp peak centered at 2.18 eV and a shoulder at 2.64 eV, the other one has three resolved peaks centered at 3.86, 4.21, and 4.43 eV, respectively. The spectrum of $C_6S_2^-$ exhibits two major features centered at 3.45 and 4.30 eV. The feature at 3.45 eV is split into three peaks centered at 3.27, 3.51, and 3.74 eV respectively. Like C_4S^- and C_6S^- , the three peaks may be contributed by the low-lying electronic states and vibrational progressions of neutral C_6S_2 . In the spectrum of $C_7S_2^-$, there are three peaks centered at 2.62,

3.08, and 3.95 eV, respectively. The first two peaks are weaker than the third one.

3.2. Theoretical results

The optimized geometries of the low-lying isomers of C_nS^- and C_nS ($n = 2-7$) are shown in Fig. 3 and 4 with the most stable ones on the left, and those of $C_nS_2^-$ and C_nS_2 ($n = 2-7$) in Fig. 5 and 6 with the most stable structures on the left. The Cartesian coordinates of the low-lying isomers of C_nS^- and $C_nS_2^-$ ($n = 2-7$) are available in the ESI,[†] (see Table S2). The symmetries, relative energies, and theoretical VDEs and ADEs of the low-lying isomers of C_nS^- and $C_nS_2^-$ ($n = 2-7$) are listed in Table 2 along with the experimental VDEs and ADEs for comparison. All harmonic vibrational frequencies of the most stable isomers of C_nS and C_nS_2 ($n = 2-7$) are available in the ESI,[†] (see Tables S3 and S4). We have also simulated the photoelectron spectra of the low-lying isomers of C_nS^- and $C_nS_2^-$ ($n = 2-7$) based on theoretically generalized Koopmans' theorem (GKT)^{45,46} and compared the simulated spectra with the experimental results in Fig. 7. For convenience, we call the simulated spectra as density of states (DOS) spectra.⁴⁶ Each transition, as the vertical lines in the DOS spectra, corresponds to the removal of an electron from a specific molecular orbital of the cluster anion. In the simulation, the first peak associated with the HOMO was set at the position of theoretical VDE, and the other peaks associated with the deeper orbitals were shifted to higher binding energy side according to the relative energies of orbitals (ΔE_n). The values of ΔE_n were calculated using the equation: $\Delta E_n = E_{(\text{HOMO})} - E_{(\text{HOMO}-n)}$, where $E_{(\text{HOMO})}$ is the energy of the HOMO, $E_{(\text{HOMO}-n)}$ is the energy of the HOMO- n orbital from theoretical calculations. The peak associated with each orbital

was fitted with a unit-area Gaussian function of 0.2 eV full width at half maximum (FWHM).

C_nS^- and C_nS ($n = 2-7$). As for C_2S^- , the most stable isomer (2A) is a C-C-S linear structure with $C_{\infty v}$ symmetry. The calculated C-C and C-S bond lengths of isomer 2A are 1.274 and 1.641 Å respectively. The calculated VDE of isomer 2A is 2.79 eV, in excellent agreement with the experimental measurement (2.75 eV). Isomer 2B is 2.70 eV much higher than isomer 2A in energy. In Fig. 7, the simulated DOS spectrum of isomer 2A also agrees with the experimental spectrum. Therefore, we can infer that isomer 2A is the most likely structure of C_2S^- in our experiments. This is consistent with the results of Neumark and coworkers²⁵ and Riaplov *et al.*¹⁸ For the neutral C_2S , the most stable isomer 2a is also a C-C-S linear structure in the $^3\Sigma^-$ electronic state. Its C-C bond length is 1.310 Å, longer than that of C_2S^- , while its C-S bond length is 1.568 Å, shorter than that of C_2S^- . Isomer 2b can be considered as an electronic excited state ($^1\Sigma^+$) of the neutral C_2S , which contributes to the peak at 3.44 eV in the spectrum of C_2S^- and in agreement with the third electronic state ($b^1\Sigma^+$) observed by Neumark and coworkers. Its energy is higher than the ground state of C_2S by 0.88 eV, which is in accordance with the calculated result (0.77 eV) by Zhang *et al.*³⁷

The most stable structure of C_3S^- (isomer 3A) is of C_s symmetry in the $^2A'$ electronic state. It is the only non-linear structure among the most stable isomers of $C_nS_m^-$ ($n = 2-7$; $m = 1, 2$) with a $\angle C1C2C3$ angle of 177.7° and a $\angle C2C3S$ angle of 170.7° (Note that the carbon atoms are numbered from the carbon farthest from the sulfur atom). Its C1-C2, C2-C3, and C3-S bond lengths are 1.286, 1.298, and 1.603 Å respectively. The linear structure of C_3S^- is found to be a transition state with one imaginary frequency. Isomer 3B has an isosceles

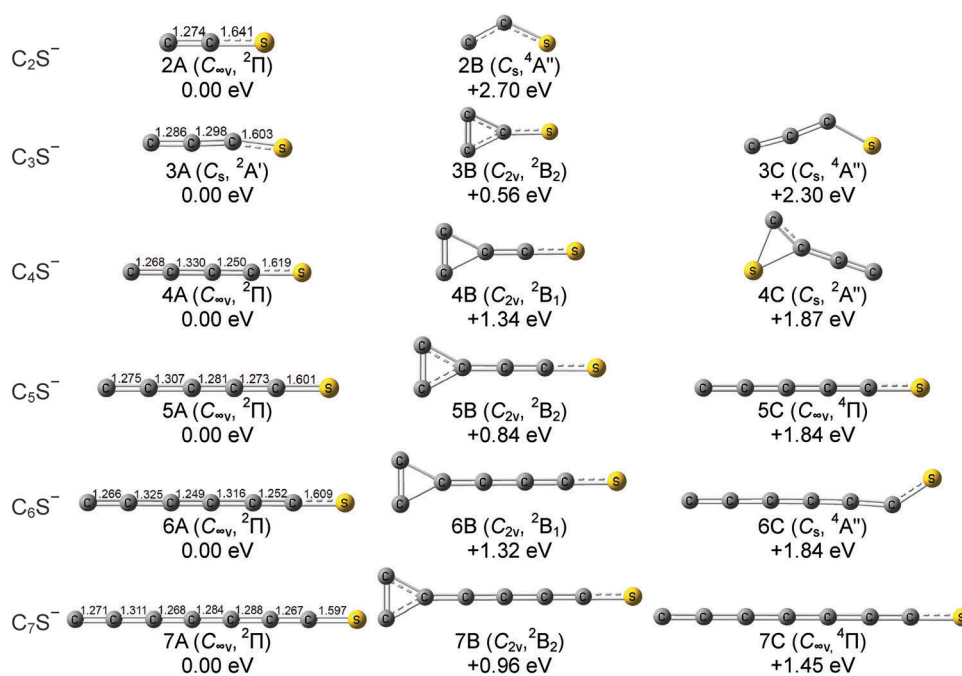


Fig. 3 Geometries, electronic states, and relative energies of the low-lying isomers of anionic C_nS^- ($n = 2-7$). The numbers above the molecular structures are bond lengths in Angstrom.

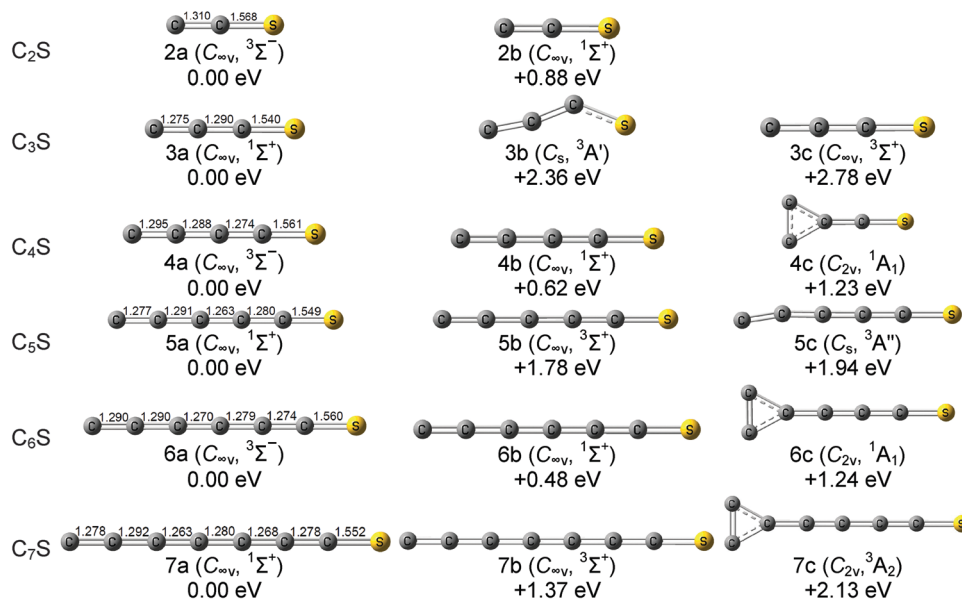


Fig. 4 Geometries, electronic states, and relative energies of the low-lying isomers of neutral C_nS ($n = 2-7$). The numbers above the molecular structures are bond lengths in Angstrom.

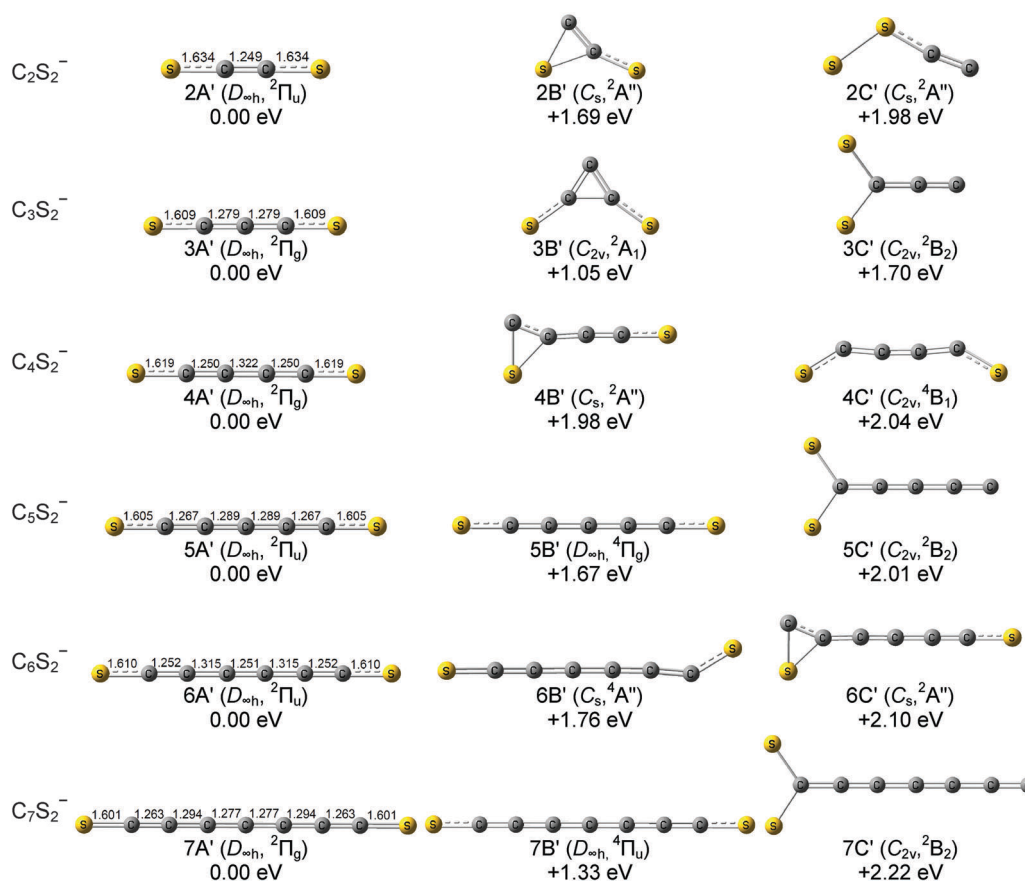


Fig. 5 Geometries, electronic states, and relative energies of the low-lying isomers of anionic $C_nS_2^-$ ($n = 2-7$). The numbers above the molecular structures are bond lengths in Angstrom.

triangle C_3 and with the S atom binding to the C atom at the vertex. The structure of isomer 3C is similar to that of isomer

3A, but having a much larger $\angle C_2C_3S$ angle than isomer 3A. Isomers 3B and 3C are much less stable than isomer 3A.

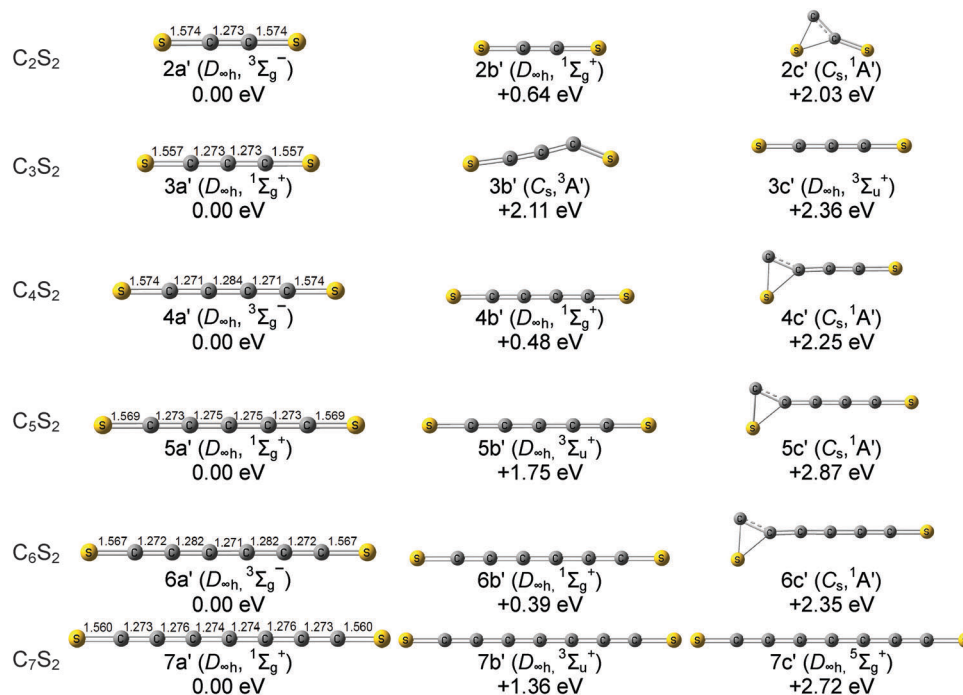


Fig. 6 Geometries, electronic states, and relative energies of the low-lying isomers of neutral C_nS_2 ($n = 2-7$). The numbers above the molecular structures are bond lengths in Angstrom.

Table 2 Relative energies, theoretical VDEs and ADEs of the low energy isomers of C_nS^- and $C_nS_2^-$ ($n = 2-7$) clusters, as well as the experimental VDEs and ADEs estimated from their photoelectron spectra. The isomers labeled in bold are the most probable isomers in the experiments

Isomer	State	Sym.	ΔE (eV)	VDE (eV)		ADE (eV)		Isomer	State	Sym.	ΔE (eV)	VDE (eV)		ADE (eV)	
				DFT	Expt.	DFT	Expt.					DFT	Expt.	DFT	Expt.
C_2S^-	2A	$^2\Pi$	0.00	2.79	2.75	2.66	2.56	$C_2S_2^-$	2A'	$^2\Pi_u$	0.00	2.44	2.58	2.29	2.27
	2B	$^4A''$	2.70	0.80		-0.04	2B'		$^2A''$	C_s	1.69	2.89		0.59	
							2C'		$^2A''$	C_s	1.98	3.54		3.43	
C_3S^-	3A	$^2A'$	0.00	1.85	1.88	1.72	1.45	$C_3S_2^-$	3A'	$^2\Pi_g$	0.00	1.57	1.58	1.44	1.26
	3B	2B_2	0.56	2.74		1.16	3B'		2A_1	C_{2v}	1.05	3.00		0.38	
	3C	$^4A''$	2.30	1.89		1.79	3C'		2B_2	C_{2v}	1.70	4.38		3.51	
C_4S^-	4A	$^2\Pi$	0.00	3.26	3.32	3.14	3.23	$C_4S_2^-$	4A'	$^2\Pi_g$	0.00	2.88	3.00	2.73	2.79
	4B	2B_1	1.34	3.24		3.03	4B'		$^2A''$	C_s	1.98	3.23		0.75	
	4C	$^2A''$	1.87	3.66		1.25	4C'		4B_1	C_{2v}	2.04	1.77		0.69	
C_5S^-	5A	$^2\Pi$	0.00	2.54	2.47	2.46	2.29	$C_5S_2^-$	5A'	$^2\Pi_u$	0.00	2.23	2.18	2.13	1.99
	5B	2B_2	0.84	3.17		1.61	5B'		$^4\Pi_g$	$D_{\infty h}$	1.67	2.29		2.21	
	5C	$^4\Pi$	1.84	2.47		2.41	5C'		2B_2	C_{2v}	2.01	4.64		3.91	
C_6S^-	6A	$^2\Pi$	0.00	3.58	3.65	3.45	3.61	$C_6S_2^-$	6A'	$^2\Pi_u$	0.00	3.20	3.27	3.05	3.18
	6B	2B_1	1.32	3.53		3.37	6B'		$^4A''$	C_s	1.76	1.89		1.29	
	6C	$^4A''$	1.84	2.29		1.59	6C'		$^2A''$	C_s	2.10	3.51		3.30	
C_7S^-	7A	$^2\Pi$	0.00	3.01	2.93	2.94	2.93	$C_7S_2^-$	7A'	$^2\Pi_g$	0.00	2.69	2.62	2.59	2.44
	7B	2B_2	0.96	3.49		1.97	7B'		$^4\Pi_u$	$D_{\infty h}$	1.33	2.70		2.62	
	7C	$^4\Pi$	1.45	3.04		2.86	7C'		2B_2	C_{2v}	2.22	4.78		4.69	

The theoretical VDE of isomer 3A is calculated to be 1.85 eV, which is consistent with the experimental value (1.88 eV). The simulated DOS spectrum of isomer 3A is also in good agreement with the experimental spectrum of C_3S^- . Thus, we suggest that isomer 3A is the most probable one detected in our

experiments. The results of C_3S^- obtained in this work are all consistent with the results reported by Neumark and coworkers.²⁶ For the neutral C_3S , the most stable isomer 3a is a C-C-C-S linear structure in the $^1\Sigma^+$ electronic state. The two C-C and one C-S bond lengths are 1.275, 1.290, and 1.540 Å respectively,

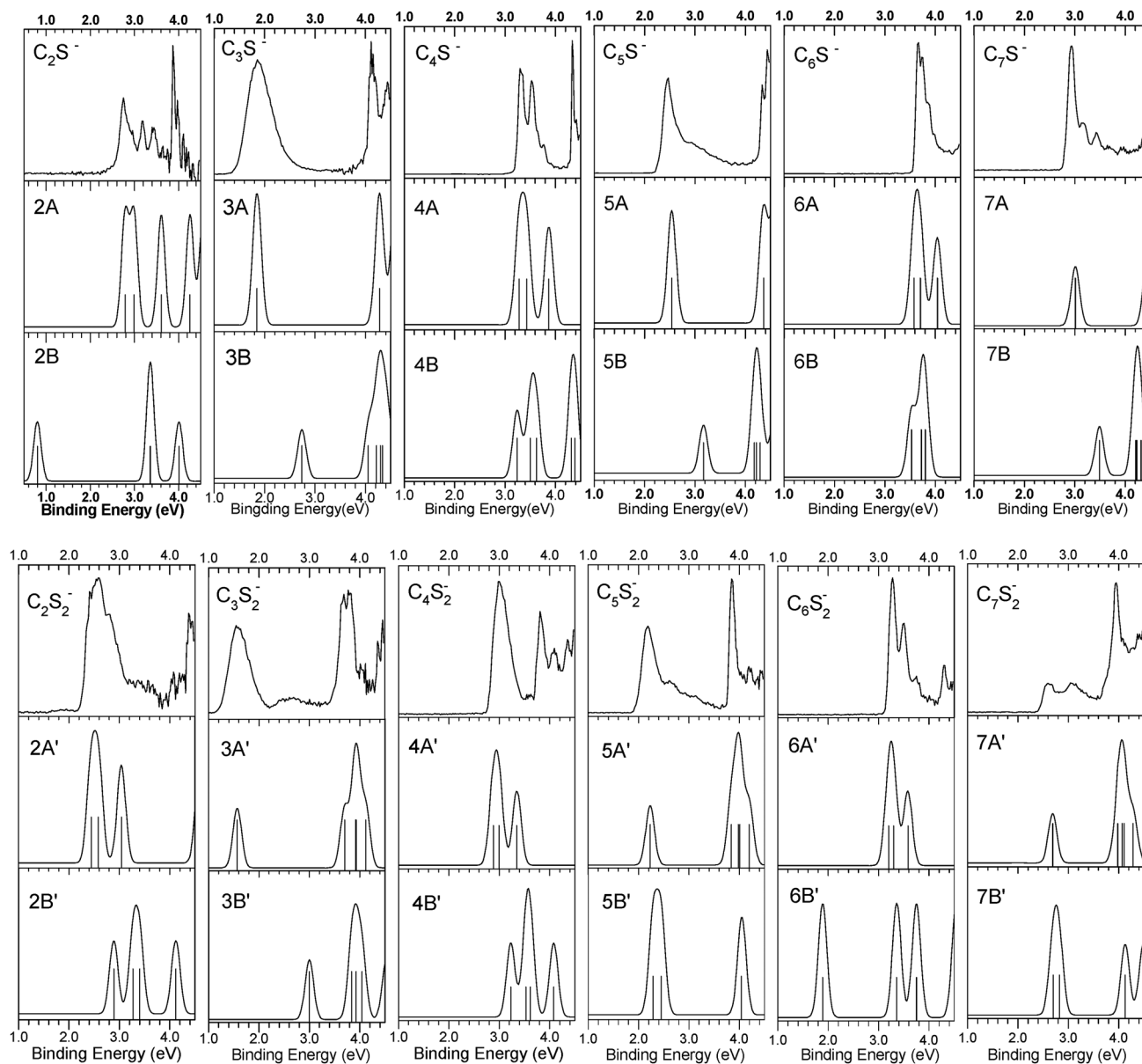


Fig. 7 Comparison of the experimental photoelectron spectra of C_nS^- and $C_nS_2^-$ ($n = 2-7$) clusters with their simulated DOS spectra. The simulations were conducted by fitting the distribution of the transition lines with unit-area Gaussian functions of 0.2 eV full width at half maximum. The vertical lines are the theoretical simulated spectral lines of C_nS^- and $C_nS_2^-$ ($n = 2-7$) clusters.

all shorter than the corresponding bond lengths of isomer 3A. The large geometry difference between C_3S^- and C_3S is consistent with the broad band in the spectrum of C_3S^- . Isomer 3b has a C–C–S bent structure with C_s symmetry. Isomer 3c can be considered as an electronic excited state of neutral C_3S . Its energy is higher than isomer 3a by 2.78 eV, corresponding to the high binding energy feature at 4.42 eV in the spectrum of C_3S^- . This is also in excellent agreement with the calculated result (2.74 eV) by Zhang *et al.*³⁶ and the value (2.78 eV) calculated by Zaidi *et al.*⁴⁷

For C_4S^- , the most stable isomer (4A) is of $C_{\infty v}$ symmetry with the S atom locating at one end of the carbon chain. Isomer 4B with C_{2v} symmetry can be obtained from isomer 3B by

inserting an additional C atom into the C=S bond. Isomer 4C has a C_2S triangle and with a C=C bond binding to one of the two C atoms of the C_2S triangle. The theoretical VDE of isomer 4A is 3.26 eV, in good agreement with the experimental measurement (3.32 eV). The simulated DOS spectrum of isomer 4A fits the experimental spectrum very well. Although the calculated VDE (3.24 eV) of isomer 4B agrees with the experimental value, it cannot exist in our experiments due to its high energy. Isomer 4C is 1.87 eV much higher than 4A in energy and its VDE (3.66 eV) is much higher than the experimental value. Therefore, isomer 4A is what we observed in our experiments. As shown in Fig. 7, the DOS spectrum of C_4S^- displays the transitions from some low-lying electronic states, indicating

that the first three peaks in the experimental spectrum of C_4S^- may be mainly contributed by the low-lying electronic states and with some minor contribution from the vibrational progressions of neutral C_4S . For neutral C_4S , isomers 4a and 4b are both C–C–C–S linear structures in $^3\Sigma^-$ and $^1\Sigma^+$ electronic states, respectively. Isomer 4b can be considered as an electronic excited state of C_4S . Its energy is 0.62 eV higher than that of isomer 4a, which is consistent with the spectral feature at 3.76 eV in Fig. 2 and the theoretical value (0.54 eV) calculated by Zhang *et al.*³⁷ Isomer 4c with C_{2v} symmetry is similar to the structure of isomer 4B.

Isomer 5A is the most stable one for C_5S^- , which is a linear structure. Isomer 5B with C_{2v} symmetry can be obtained from isomer 4B by inserting an additional C atom into the C=S bond. Isomer 5C is similar to the structure of isomer 5A in the $^4\Pi$ electronic state. The theoretical VDE of isomer 5A is calculated to be 2.54 eV, which is consistent with the experimental value (2.47 eV). The simulated DOS spectrum of isomer 5A is also in good agreement with the photoelectron spectrum of C_5S^- . The energies of isomers 5B and 5C are higher than isomer 5A by 0.84 and 1.84 eV, respectively. Thus, we can infer that isomer 5A is the most likely structure for C_5S^- . For the neutral C_5S , isomers 5a and 5b are both linear structures in $^1\Sigma^+$ and $^3\Sigma^+$ electronic states, respectively. Isomer 5b is an electronic excited state of neutral C_5S , which contributes to the high binding energy band at 4.34 eV in the spectrum of C_5S^- . Its energy is 1.78 eV higher than that of isomer 5a, which is in accordance with the calculated value (1.88 eV) by Zhang *et al.*³⁶ Isomer 5c is a nonlinear structure with a bend of the terminal C=C bond.

As for C_6S^- , the most stable isomer (6A) is a linear structure with a terminal S atom. Isomer 6B with C_{2v} symmetry can be obtained from isomer 5B by inserting an additional C atom into the C=S bond. Isomer 6C is a nonlinear structure with a bend of the terminal C=S bond. The calculated VDE (3.58 eV) of isomer 6A agrees with the experimental value (3.65 eV). The simulated DOS spectrum of isomer 6A is also consistent with the experimental spectrum. Isomers 6B and 6C are much less stable than isomer 6A. Therefore, the existence of isomers 6B and 6C can be ruled out. Isomer 6A is the most probable one detected in our experiments. As we can see from Fig. 7, the DOS spectrum of C_6S^- presents the transitions from some low-lying electronic states, indicating that the four peaks in the experimental spectrum of C_6S^- may be mainly contributed by the low-lying electronic states and with some minor contribution from the vibrational progressions of neutral C_6S . For the neutral C_6S , its ground state structure (6a) is linear with a terminal C=S bond. We find an electronic excited state ($^1\Sigma^+$) of neutral C_6S (isomer 6b), which is higher than the ground state of C_6S by 0.48 eV in energy, and in reasonable agreement with the calculated result (0.30 eV) by Zhang *et al.*³⁷ The structure of isomer 6c is similar to that of isomer 6B, which includes an isosceles triangle C_3 and a C–C–C–S linear chain.

We displayed three low-lying isomers for C_7S^- . Isomer 7A is a $C_{\infty v}$ symmetric linear structure with a terminal C=S bond. Isomer 7B with C_{2v} symmetry can be obtained from isomer 6B

by inserting an additional C atom into the C=S bond. The energy of isomer 7B is higher than that of isomer 7A by 0.96 eV, and its theoretical VDE (3.49 eV) is very different from our experimental result (2.93 eV). Isomer 7C is a linear structure in the $^4\Pi$ electronic state. Its energy is higher than that of isomer 7A by 1.45 eV. The calculated VDE of isomer 7A is 3.01 eV, in excellent agreement with the experimental measurement. In Fig. 7, we can see that the simulated DOS spectrum of isomer 7A fits well with the experimental spectrum of C_7S^- . Thus, we suggest that isomer 7A is the most likely structure for C_7S^- in our experiments. For the neutral C_7S , isomers 7a and 7b is similar to the structure of isomer 7A, which is a linear structure with a terminal S atom. The calculated vibrational frequency of the neutral C_7S is 2084 cm^{-1} (scaled by a factor of 0.9510⁴⁴), which is in good agreement with the corresponding vibrational separation of 2016 cm^{-1} observed experimentally in this work and the calculated result (2111 cm^{-1}) by Wang *et al.*²⁹ Isomer 7b can be considered as an electronic excited state of the neutral C_7S , which contributes to the high binding energy band beyond 4.3 eV in the spectrum of C_7S^- . Its energy is 1.37 eV higher than that of isomer 7a, which is consistent with the calculated result (1.43 eV) by Zhang *et al.*³⁶ Isomer 7c can be obtained from isomer 6a by inserting an additional C atom into the terminal C=S bond.

$C_nS_2^-$ and C_nS_2 ($n = 2-7$). The most stable isomer of $C_2S_2^-$ (isomer 2A') is a S–C–C–S linear structure with the C–S bond length of 1.634 Å and the C–C bond length of 1.249 Å. Isomer 2B' has a C_2S triangle and with an additional S atom binding to one C atom. Isomer 2C' is an S–S–C–C bent structure with C_s symmetry. The calculated VDE (2.44 eV) of isomer 2A' is in agreement with the experimental measurement (2.58 eV). In Fig. 7, we can see that the simulated DOS spectrum of isomer 2A' fits well with the experimental spectrum of $C_2S_2^-$. The energies of isomers 2B' and 2C' are much higher than that of isomer 2A' by 1.69 and 1.98 eV, respectively. Therefore, the existence of isomers 2B' and 2C' in our experiments can be ruled out. Isomer 2A' is the most probable one detected in our experiments. For the neutral C_2S_2 , the structure of the most stable isomer (2a') is similar to that of isomer 2A', in which the C–S bond length is shorter than that of isomer 2A' by 0.060 Å, and the C–C bond length is longer than that of isomer 2A' by 0.024 Å. Isomer 2b' is also similar to the structure of isomer 2A'. Isomer 2c' is similar to the structure of isomer 2B' with C_s symmetry.

The most stable isomer (3A') is a S–C–C–C–S linear structure with $D_{\infty h}$ symmetry, in which the C–S and C–C bond lengths are 1.609 Å and 1.279 Å, respectively. Isomer 3B' has an isosceles triangle C_3 and with two S atoms binding to the bottom two carbon atoms respectively. Isomer 3C' is a Y-shaped structure with C_{2v} symmetry. The theoretical VDE of isomer 3A' is 1.57 eV, in excellent agreement with the experimental value (1.58 eV). The simulated DOS spectrum of isomer 3A' is also consistent with the experimental spectrum. The calculated VDEs of isomers 3B' and 3C' are 3.00 and 4.38 eV respectively, which both deviate from our experimental result. The energies of isomers 3B' and 3C' are much higher than isomer 3A' by 1.05 and 1.70 eV, respectively.

Thus, we can exclude the existence of isomers 3B' and 3C'. Isomer 3A' is what we observed in our experiments. For C_3S_2 neutral, isomers 3a' and 3c' have similar structures in different electronic states, similar to the structure of isomer 3A'. The C–S bond length of isomer 3a' is 1.557 Å, shorter than that of isomer 3A' by 0.052 Å, and the C–C bond length is 1.273 Å, close to that of isomer 3A'. Isomer 3b' is a S–C–C–S bent structure with a $\angle CCS$ angle of 144° , which can be viewed as an electronic excited state of C_3S_2 . Its energy is 2.11 eV higher than that of isomer 3a', which is consistent with the spectral band centered at 3.74 eV in Fig. 2.

For $C_4S_2^-$, the most stable isomer (4A') is a linear structure with two S atoms locating at two ends of the carbon chain. Isomer 4B' has a C_2S triangle with a linear chain of C_2S binding to one C atom of the C_2S triangle. Isomer 4C' is of C_{2v} symmetry with two terminal C=S bonds bending toward the same side of the carbon chain. The energies of isomers 4B' and 4C' are much higher than that of isomer 4A' by 1.98 and 2.04 eV respectively. The calculated VDE (2.88 eV) of isomer 4A' is in agreement with the experimental value (3.00 eV). In Fig. 7, the simulated DOS spectrum of isomer 4A' is also consistent with the experimental spectrum. Therefore, isomer 4A' is the most likely structure for $C_4S_2^-$. For the neutral C_4S_2 , the structures of isomers 4a' and 4b' are both linear with two terminal C=S bonds. Isomer 4b' is higher than isomer 4a' by 0.48 eV in energy, which is an electronic excited state of neutral C_4S_2 and consistent with the spectral feature at 3.60 eV in the spectrum of $C_4S_2^-$. The structure of isomer 4c' is similar to that of isomer 4B' with C_s symmetry.

We displayed three low-lying isomers for $C_5S_2^-$. Isomers 5A' and 5B' are both linear structures with two terminal C=S bonds in different electronic states. The energy of isomer 5B' is 1.67 eV higher than that of isomer 5A'. Isomer 5C' is a Y-shaped structure with a linear chain of C_5 . The theoretical VDE of isomer 5C' is 4.64 eV, which deviates from our experimental measurement (2.18 eV). The calculated VDE of isomer 5A' is 2.23 eV, in good agreement with the experimental value. The simulated DOS spectrum of isomer 5A' fits the experimental spectrum very well. Thus, we suggest isomer 5A' to be the most probable one detected in our experiments. For neutral C_5S_2 , the first two low-lying isomers (5a' and 5b') are both linear structures in different electronic states. Isomer 5c' has a C_2S triangle with a linear chain of C_3S binding to one C atom of the C_2S triangle. The energies of isomers 5b' and 5c' are 1.75 and 2.87 eV higher than isomer 5a', respectively. Isomer 5b' is an electronic excited state of neutral C_5S_2 , which contributes to the peak at 3.86 eV in the spectrum of $C_5S_2^-$.

For $C_6S_2^-$, we displayed three low-lying isomers. The most stable isomer (6A') is a linear structure, which can be obtained from isomer 5A' by inserting an additional C atom into the C=C bond. Isomer 6B' is a nonlinear structure with the bend of one terminal C=S bond. Isomer 6C' has a C_2S triangle with a C_4S linear chain binding to one C atom of the C_2S subunit. The calculated VDE (3.20 eV) of isomer 6A' is consistent with the experimental result (3.27 eV). In Fig. 7, we can see that the simulated DOS spectrum of isomer 6A' fits well with the experimental spectrum of $C_6S_2^-$. The existence of isomers 6B'

and 6C' can be ruled out due to their high energy. Thus, isomer 6A' is observed in our experiments. As shown in Fig. 7, the DOS spectrum of $C_6S_2^-$ displays some low-lying electronic state transitions, indicating that the first three peaks in the experimental spectrum of $C_6S_2^-$ may be mainly contributed by the low-lying electronic states and with some minor contribution from the vibrational progressions of neutral C_6S_2 . For the neutral C_6S_2 , the first two isomers 6a' and 6b' are both linear structures with $D_{\infty h}$ symmetry in different electronic states. The energy of isomer 6b' is higher than that of isomer 6a' by 0.39 eV. Isomer 6b' can be viewed as an electronic excited state of neutral C_6S_2 , which is in agreement with the spectral peak at 3.74 eV in Fig. 2. The structure of isomer 6c' is similar to that of isomer 6C'.

The structures of isomers 7A' and 7B' are both linear with two terminal C=S bonds. The energy of isomer 7B' is 1.33 eV higher than isomer 7A'. Isomer 7C' is a Y-shaped structure with a carbon chain of C_7 , and higher in energy than isomer 7A' by 2.22 eV. The calculated VDE of isomer 7A' is 2.69 eV, in good agreement with the experimental value (2.62 eV). The simulated DOS spectrum of isomer 7A' is also consistent with the experimental spectrum of $C_7S_2^-$. Although the theoretical VDE (2.70 eV) of isomer 7B' is in agreement with the experimental result, it cannot exist in our experiments due to its high energy. Isomer 7C' can also be ruled out because of its high energy and large theoretical VDE (4.78 eV). Therefore, we suggest that isomer 7A' is the most probable one observed in our experiments. As we can see from the simulated DOS spectrum of isomer 7A', there is only one electronic state at the low electron binding energy side, therefore, the first two peaks in the $C_7S_2^-$ spectrum belong to one electronic state, which probably includes several unresolved vibrational states. For the neutral C_7S_2 , three low-lying isomers are all linear structures with two terminal C=S bonds in different electronic states. The energies of isomers 7b' and 7c' is higher than that of isomer 7a' by 1.36 and 2.72 eV, respectively. Isomer 7b' can be considered as an electronic excited state of neutral C_7S_2 , which is in accordance with the peak at 3.95 eV in the spectrum of $C_7S_2^-$.

3.3. Discussion

Fig. 8 shows the change in experimental and theoretical VDEs versus the number of carbon atoms. It can be seen that the calculated VDEs are in good agreement with the experimental VDEs. The VDEs of C_nS^- clusters are higher than those of $C_nS_2^-$ clusters with the same n . It is interesting that the VDEs of both C_nS^- and $C_nS_2^-$ ($n = 2-7$) exhibit very obvious odd–even alternation: the VDEs of even- n clusters are larger than those of adjacent odd- n clusters. And for C_nS^- and $C_nS_2^-$ in both odd and even series, the VDEs increase with increasing n . Why the VDEs of even- n clusters are higher than those of adjacent odd- n clusters? As we all know, the ground state of neutral C_2S has an open-shell electronic configuration π^2 , giving rise to a $^3\Sigma^-$ electronic state, while the ground state of neutral C_3S has a close-shell electronic configuration π^4 , forming a $^1\Sigma^+$ electronic state. When the anionic C_2S^- is formed, the excess electron is added into a half-occupied π -orbital; while for the formation of

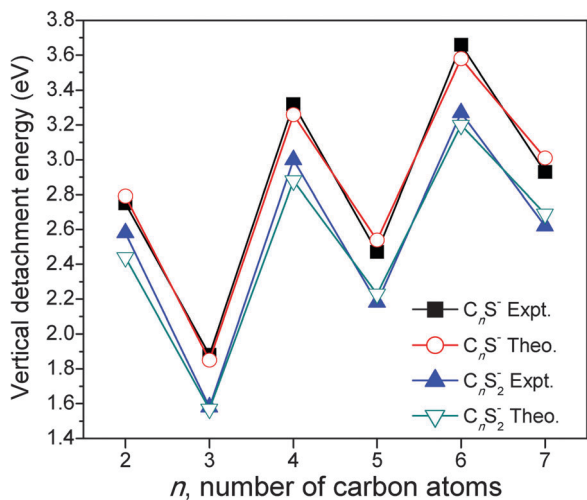


Fig. 8 Experimental and theoretical VDEs of C_nS^- and $C_nS_2^-$ ($n = 2-7$) clusters versus n , the number of carbon atoms.

C_3S^- , the excess electron is added into an empty anti-bonding π^* -orbital which is higher than the π -orbitals in energy. Therefore, the VDE of C_2S^- is larger than that of C_3S^- . According to the above discussion, we can infer that the VDEs of C_nS^- with even n are larger than those of adjacent C_nS^- with odd n because the corresponding neutrals of the even-numbered clusters have open-shell electronic structures with half-occupied π -orbitals while those of the odd-numbered clusters have close-shell electronic structures with fully-occupied π -orbitals, which are consistent with those observed experimentally in this work. Similar to C_nS^- , the VDEs of even- n $C_nS_2^-$ are larger than those of adjacent odd- n $C_nS_2^-$ because even- n C_nS_2 clusters all have π^2 electronic configuration, while odd- n C_nS_2 clusters have π^4 electronic configuration. In addition, as we can see from the photoelectron spectra of C_nS^- and $C_nS_2^-$, the HOMO-LUMO gaps of the spectra with odd n are larger than those of the spectra with even n , which is because the neutral C_nS and C_nS_2 clusters with odd n are all close-shell with $^1\Sigma^+$ and $^1\Sigma_g^+$ electronic ground states respectively. Based on that, we can ensure that the first feature of the photoelectron spectrum of C_7S^- belongs to the resolved vibrational peaks of the ground state of the neutral C_7S , instead of the different electronic states. This point can also be confirmed by the simulated DOS spectrum of C_7S^- , in which there is only one electronic state in the low binding energy side.

Because the most stable structures of C_nS_m ($n = 2-7$; $m = 1, 2$) are similar to those of the corresponding anions with the exception of C_3S , the measured ADE values of anionic clusters can be considered as equal to the EAs of their corresponding neutrals. Hence, we estimated the EAs of neutral C_nS ($n = 2, 4-7$) to be 2.56, 3.23, 2.29, 3.61 and 2.93 eV respectively, and the EAs of neutral C_nS_2 ($n = 2-7$) to be 2.27, 1.26, 2.79, 1.99, 3.18, and 2.44 eV respectively based on the ADEs of their corresponding anions. The ADE of the C_3S^- anion cannot be viewed as the EA of neutral C_3S due to the large structural difference between the anionic and neutral C_3S .

It would be interesting to compare the structures of C_nS_m ($m = 1, 2$) clusters with their isoelectronic counterparts such as C_nO_m and Si_nS_m ($m = 1, 2$) clusters which were investigated previously by a number of experiments and theoretical calculations. The most stable structures of the neutral C_nO ($n \leq 9$)⁴⁸⁻⁵¹ and C_nO_2 ($n = 2-7$)⁵²⁻⁵⁹ clusters reported in the literature are similar to those of corresponding neutral C_nS and C_nS_2 , they are all linear configurations with a carbon chain C_n terminated either by the O/S atom at one end or at both ends. This is because that the oxygen atom and the sulfur atom have similar bonding characteristics. The experimental measurements and theoretical calculations suggested that the lowest-energy structures of the neutral Si_nS_m ($m = 1, 2$) clusters with $n > 1$ are all nonlinear configurations. The most stable structures of Si_2S and Si_2S_2 are both cyclic structures.⁶⁰ The Si_4S is a tetragonal pyramidal, Si_5S a pentagonal structure with five Si atoms forming a pentagon with one S atom in the centre of the pentagon, and Si_4S_2 a tetragonal bipyramidal structure with two sulfur atoms locating on the opposite sides of the silicon square.⁶¹ They are very different from the linear structures of C_nS and C_nS_2 . The structural differences between carbon-sulfur and silicon-sulfur clusters are probably because the two carbon atoms prefer to form bonds with each other *via* sp^2 hybridization while the silicon atoms prefer sp^3 hybridization.

4. Conclusions

Binary cluster anions composed of carbon and sulfur atoms, C_nS^- and $C_nS_2^-$ ($n = 2-7$), were investigated in combination with photoelectron spectroscopy and DFT calculations. The VDEs of C_nS^- and $C_nS_2^-$ both display an obvious parity effect with an increasing number of carbon atoms. The most probable ground-state isomers of $C_nS_m^-$ ($n = 2-7$; $m = 1, 2$) were determined by comparing the calculated VDEs with the experimental results. The results show that the anionic and neutral C_nS ($n = 2-7$) clusters are linear configurations with the S atom locating at one end of the carbon chain except that the structure of C_3S^- is slightly bent. The anionic and neutral C_nS_2 ($n = 2-7$) are all linear structures with two S atoms locating at two ends of the carbon chain. We obtained the EAs of neutral C_nS ($n = 2, 4-7$) and C_nS_2 ($n = 2-7$) based on the experimental ADEs of the corresponding anionic species because the most stable structures of the anionic and neutral clusters are similar.

Acknowledgements

This work was supported by the Natural Science Foundation of China (Grant No. 21303214 and 21273246) and the Knowledge Innovation Program of the Chinese Academy of Sciences (Grant No. KJJCX2-EW-H01). The theoretical calculations were conducted on the ScGrid and DeepComp 7000 of the Supercomputing Center, Computer Network Information Center of Chinese Academy of Sciences.

References

- 1 S. Klinge, J. Hirst, J. D. Maman, T. Krude and L. Pellegrini, *Nat. Struct. Mol. Biol.*, 2007, **14**, 875.
- 2 G. Andre, S. Even, H. Putzer, P. Burguiere, C. Croux, A. Danchin, I. MartinVerstraete and O. Soutourina, *Nucleic Acids Res.*, 2008, **36**, 5955.
- 3 S. P. Souza and B. L. Lutz, *Astrophys. J.*, 1977, **216**, L49–L51.
- 4 K. H. Hinkle, J. J. Keady and P. F. Bernath, *Science*, 1988, **241**, 1319–1322.
- 5 P. F. Bernath, K. H. Hinkle and J. J. Keady, *Science*, 1989, **244**, 562–564.
- 6 J. Cami, J. Bernard-Salas, E. Peeters and S. E. Malek, *Science*, 2010, **329**, 1180–1182.
- 7 A. A. Penzias, P. M. Solomon, R. W. Wilson and K. B. Jefferts, *Astrophys. J.*, 1971, **168**, L53–L58.
- 8 B. Zuckerman, M. Morris, P. Palmer and B. E. Turner, *Astrophys. J.*, 1972, **173**, L125–L129.
- 9 J. Cernicharo, M. Gurlin, H. Hein and C. Kahne, *Astron. Astrophys.*, 1987, **181**, L9–L12.
- 10 N. Kaifu, H. Suzuki, M. Ohishi and T. Miyaji, *Astrophys. J.*, 1987, **317**, L111–L114.
- 11 S. Saito, K. Kawaguchi, S. Yamamoto, M. Ohishi, H. Suzuki and N. Kaifu, *Astrophys. J.*, 1987, **317**, L115–L119.
- 12 S. Yamamoto, S. Saito, K. Kawaguchi, N. Kaifu, H. Suzuki and M. Ohishi, *Astrophys. J.*, 1987, **317**, L119–L121.
- 13 M. B. Bell, L. W. Avery and P. A. Feldman, *Astrophys. J.*, 1993, **417**, L37–L40.
- 14 M. Agúndez, J. Cernicharo and M. Guélin, *Astron. Astrophys.*, 2014, **570**, A45.
- 15 M. Ikeda, Y. Sekimoto and S. Yamamoto, *J. Mol. Spectrosc.*, 1997, **185**, 21–25.
- 16 Y. Ohshima and Y. Endo, *J. Mol. Spectrosc.*, 1992, **153**, 627–634.
- 17 J. Tang and S. Saito, *J. Mol. Spectrosc.*, 1995, **169**, 92–107.
- 18 E. Riaplov, M. Wyss, J. P. Maier, D. Panten, G. Chambaud, P. Rosmus and J. Fabian, *J. Mol. Spectrosc.*, 2003, **222**, 15–21.
- 19 G. Maier, Hans P. Reisenauer and R. Ruppel, *Eur. J. Org. Chem.*, 2004, 4197–4202.
- 20 G. Maier, J. Schrot, H. P. Reisenauer and R. Janoschek, *Chem. Ber.*, 1991, **124**, 2617.
- 21 A. J. Schoeffler, H. Kohguchi, K. Hoshina, Y. Ohshima and Y. Endo, *J. Chem. Phys.*, 2001, **114**, 6142.
- 22 M. Nakajima, Y. Sumiyoshi and Y. Endo, *J. Chem. Phys.*, 2002, **117**, 9327.
- 23 J. Szczepanski, R. Hodyss, J. Fuller and M. Vala, *J. Phys. Chem. A*, 1999, **103**, 2975–2981.
- 24 H. Y. Wang, J. Szczepanski, A. Cooke, P. Brucat and M. Vala, *Int. J. Quantum Chem.*, 2005, **102**, 806–819.
- 25 E. Garand, T. I. Yacovitch and D. M. Neumark, *J. Chem. Phys.*, 2008, **129**, 074312.
- 26 E. Garand, T. I. Yacovitch and D. M. Neumark, *J. Chem. Phys.*, 2009, **131**, 054312.
- 27 S. H. Yang, C. L. Pettiette, J. Conceicao, O. Cheshnovsky and R. E. Smalley, *Chem. Phys. Lett.*, 1987, **139**, 233–238.
- 28 S. H. Yang, K. J. Taylor, M. J. Craycraft, J. Conceicao, C. L. Pettiette, O. Cheshnovsky and R. E. Smalley, *Chem. Phys. Lett.*, 1988, **144**, 431–436.
- 29 H. Wang, J. Szczepanski, P. Brucat and M. Vala, *Int. J. Quantum Chem.*, 2005, **102**, 795–805.
- 30 G. Pascoli and H. Lavendy, *Int. J. Mass Spectrom.*, 1998, **181**, 11–25.
- 31 G. Pascoli and H. Lavendy, *Int. J. Mass Spectrom.*, 1998, **181**, 135–149.
- 32 Z. C. Tang and J. J. Belbruno, *Int. J. Mass Spectrom.*, 2001, **208**, 7–16.
- 33 S. Lee, *Chem. Phys. Lett.*, 1997, **268**, 69–75.
- 34 K.-H. Kim, B. Lee and S. Lee, *Chem. Phys. Lett.*, 1998, **297**, 65–71.
- 35 I. Pérez-Juste, A. M. Graña, L. Carballeira and R. A. Mosquera, *J. Chem. Phys.*, 2004, **121**, 10447–10455.
- 36 J. L. Zhang, W. P. Wu, L. B. Wang, X. Chen and Z. X. Cao, *J. Phys. Chem. A*, 2006, **110**, 10324–10329.
- 37 J. Zhang, W. Wu, L. Wang and Z. Cao, *J. Chem. Phys.*, 2006, **124**, 124319.
- 38 H.-G. Xu, Z.-G. Zhang, Y. Feng, J. Y. Yuan, Y. C. Zhao and W. J. Zheng, *Chem. Phys. Lett.*, 2010, **487**, 204–208.
- 39 C. Lee, W. Yang and R. G. Parr, *Phys. Rev. B: Condens. Matter Mater. Phys.*, 1988, **37**, 785–789.
- 40 A. D. Becke, *J. Chem. Phys.*, 1993, **98**, 5648.
- 41 J. A. Pople, M. Head-Gordon and K. Raghavachari, *J. Chem. Phys.*, 1987, **87**, 5968.
- 42 T. H. Dunning, *J. Chem. Phys.*, 1989, **90**, 1007.
- 43 M. J. Frisch, G. W. Trucks and H. B. Schlegel, *et al.*, *Gaussian 09, Revision A. 02*, Gaussian, Inc., Wallingford, CT, 2009.
- 44 H. Y. Wang, J. Szczepanski, P. J. Brucat and M. T. Vala, *J. Phys. Chem. A*, 2003, **107**, 10919–10925.
- 45 D. J. Tozer and N. C. Handy, *J. Chem. Phys.*, 1998, **109**, 10180.
- 46 J. Akola, M. Manninen, H. Häkkinen, U. Landman, X. Li and L.-S. Wang, *Phys. Rev. B: Condens. Matter Mater. Phys.*, 1999, **60**, R11297–R11300.
- 47 A. Zaidi, S. Lahmar, Z. B. Lakhdar, P. Rosmus and M. Hochlaf, *Theor. Chem. Acc.*, 2005, **114**, 341–349.
- 48 N. Moazzen-Ahmadi and F. Zerbetto, *J. Chem. Phys.*, 1995, **103**, 6343.
- 49 T. Ogata, Y. Ohshima and Y. Endo, *J. Am. Chem. Soc.*, 1995, **117**, 3593–3598.
- 50 Y. Ohshima, Y. Endo and T. Ogata, *J. Chem. Phys.*, 1995, **102**, 1493.
- 51 E. Riaplov, M. Wyss, N. M. Lakin and J. P. Maier, *J. Phys. Chem. A*, 2001, **105**, 4894–4897.
- 52 D. Talbi and G. S. Chandler, *J. Phys. Chem. A*, 2000, **104**, 5872–5881.
- 53 S. Bell, T. S. Varadarajan, A. D. Walsh, P. A. Warsop, J. Lee and L. Sutcliffe, *J. Mol. Spectrosc.*, 1966, **21**, 42–47.
- 54 G. Maier, H. P. Reisenauer, H. Balli, W. Brandt and R. Janoschek, *Angew. Chem.*, 1990, **102**, 920–923.
- 55 G. Maier, H. P. Reisenauer, U. Schafer and H. Balli, *Angew. Chem.*, 1988, **100**, 590–592.

- 56 F. Holland, M. Winnewisser, G. Maier, H. P. Reisenauer and A. Ulrich, *J. Mol. Spectrosc.*, 1988, **130**, 470–474.
- 57 D. Strelnikov, R. Reusch and W. Kratschmer, *J. Phys. Chem. A*, 2006, **110**, 12395–12399.
- 58 G. Maier, H. P. Reisenauer and A. Ulrich, *Tetrahedron Lett.*, 1991, **32**, 4469–4472.
- 59 A. R. Dixon, T. Xue and A. Sanov, *Angew. Chem., Int. Ed.*, 2015, **54**, 8764–9767.
- 60 X. L. Xu, X. J. Deng, H. G. Xu and W. J. Zheng, *J. Chem. Phys.*, 2014, **141**, 124310.
- 61 V. R. Devi, N. A. Zabidi and K. N. Shrivastava, *Mater. Chem. Phys.*, 2013, **141**, 651–656.